Synthesis and Properties of Poly(methyl methacrylate)/Carbon Nanotube Composites Covalently Integrated Through *In Situ* Radical Polymerization

Liqiang Cui,[1,2] Naresh H. Tarte,[1] Seong Ihl Woo[1]

[1]*Department of Chemical and Biomolecular Engineering and Center for Ultramicrochemical Process System, Korea Advanced Institute of Science and Technology, 373-1 Guseong-Dong, Yuseong-Gu, Daejeon 305-701, Republic of Korea*
[2]*College of Chemical and Environmental Engineering, Shandong University of Science and Technology, 579 Qianwangang Road Economic and Technical Development Zone, Qingdao Shandong Province, People's Republic of China*

Received 16 October 2009; accepted 14 April 2010
DOI 10.1002/app.32639
Published online 27 July 2010 in Wiley Online Library (wileyonlinelibrary.com).

ABSTRACT: Poly(methyl methacrylate) (PMMA)/single-walled carbon nanotube (SWNT) composites were synthesized by the grafting of PMMA onto the sidewalls of SWNTs via *in situ* radical polymerization. The free-radical initiators were covalently attached to the SWNTs by a well-known esterification method and confirmed by means of thermogravimetric analysis and Fourier transform infrared spectroscopy. Scanning electron microscopy and transmission electron microscopy were used to image the PMMA–SWNT composites; these images showed the presence of polymer layers on the surfaces of debundled, individual nanotubes. The PMMA–SWNT composites exhibited better solubility in chloroform than the solution-blended composite materials. On the other hand, compared to the neat PMMA, the PMMA–SWNT nanocomposites displayed a glass-transition temperature up to 6.0°C higher and a maximum thermal decomposition temperature up to 56.6°C higher. The unique properties of the nanocomposites resulted from the strong interactions between the SWNTs and the PMMA chains. © 2010 Wiley Periodicals, Inc. J Appl Polym Sci 119: 452–459, 2011

Key words: carbon nanotube; nanocomposites; radical polymerization

INTRODUCTION

Polymer nanocomposites are a new class of organic polymer materials with nanosized filler domains finely dispersed in a polymer matrix. Nanosized fillers at a few weight percentage in reinforced polymer nanocomposites strongly influence the macroscopic properties of the polymer. The resulting polymer nanocomposites can result in a significant improvement in some of their properties, such as a higher heat distortion temperatures, an enhanced flame resistance, an increased modulus, better barrier properties, a reduced thermal expansion coefficient, and altered electronic and optical properties.[1–7] Since the discovery of carbon nanotubes,[8] carbon nanotube-based polymer composites have become a focal point of nanocomposite research because of the unique properties of carbon nanotubes, including their high electrical conductivity, large aspect ratio, mechanical strength, and chemical stability.[9,10] The Young's modulus of carbon nanotubes can reach 1 Tpa,[11] whereas their strength has been measured at up to 63 Gpa.[12] This allows the fabrication of materials such as supertough polymer–nanotube composite fibers.[13]

However, single-walled carbon nanotubes (SWNTs) are very difficult to disperse in polymeric matrices because of their large surface area and van der Waals forces, which can lead to the formation of strongly bound nanotube aggregates.[14] Various methods, including the solution mixing of polymer and SWNTs,[15,16] melt blending[17] and the use of surfactants to aid dispersion,[18] to obtain the homogeneous and efficient dispersion of SWNTs in the polymer matrix have been investigated. The use of functionalized SWNTs to improve the mechanical properties in polymer/SWNT composites has also been reported.[19,20] In addition, some authors have also reported the *in situ* polymerization of methyl methacrylate (MMA) monomer in the presence of pristine nanotubes.[21–26] This can result in the covalent attachment of nanotubes to the polymer via the

Correspondence to: S. I. Woo (siwoo@kaist.ac.kr).
Contract grant sponsor: Center for Ultramicrochemical Process Systems and WCU program (31-2008-000210055-0) sponsored by Korea Science and Engineering Foundation (2008).

SWNT surface π-bond opening by the initiator. However, because only a small amount of initiators can attach to the surface of SWNTs, it is not easy to achieve efficient dispersion and the formation of a strong interface between the nanotubes and the polymer matrix.

In this article, a novel method for preparing poly(methyl methacrylate) (PMMA)/SWNT nanocomposites by *in situ* polymerization is presented. Free-radical initiators with difunctional carboxyl groups were covalently attached to hydroxyl-functionalized single-walled carbon nanotubes (SWNT-OHs) by esterification. The free-radical initiators attached on the surfaces of the SWNTs were used to polymerize the MMA monomer; this resulted in the covalent attachment of the polymer on the surfaces of the carbon nanotubes. As a result, the nanotubes were debundled, and the PMMA-grafted SWNT was dispersed efficiently in the PMMA matrix. Additionally, we investigated the morphology and solubility of the PMMA–SWNT nanocomposites and their mechanical properties and thermal stability.

EXPERIMENTAL

Materials

The SWNT-OHs (length = 5–30 μm, specific surface area = 407 m^2/g) used in this study were purchased from Cheap Tubes, Inc. (Brattleboro, VT). Their purity was greater than 95 wt %, and their OH content (3.96 wt %) was confirmed by X-ray photoelectron spectroscopy. Tetrahydrofuran (THF), dimethylformamide, 4,4′-azobis(4-cyanovaleric acid) (75%), 4-(dimethylamino) pyridine (DMAP; 99%), and *N*,*N*′-dicyclohexyl carbodiimide (DCC; 99%) were purchased from Aldrich and were used as received. MMA was purchased from Aldrich (St. Louis, MO) and was distilled from CaH_2 *in vacuo.*

Preparation of the initiator-attached single-walled carbon nanotubes (SWNT-Is)

The SWNT-OHs were treated with free-radical initiators having difunctional carboxyl groups by a well-known esterification method with DCC/DMAP.[27] Typically, 0.13 g (OH content = 0.303 mmol) of SWNT-OHs was dispersed in 40 mL of dimethylformamide and sonicated for 1 h at room temperature. Carboxylic acid (0.147 g, 0.393 mmol) and DMAP (0.0033 g, 26.7 μmol) of DMAP were added to a stirred SWNT-OH suspension. DCC (0.063 g, 0.303 mmol) was added to the reaction mixture at 0°C and then stirred for 10 min at 0°C and for the next 12 h at room temperature and for 1 h with excess distilled water. The precipitate was filtered and washed with excess distilled water until the pH value reached 7.0. The final products (SWNT-Is) were collected and dried *in vacuo.* The contents of the initiator in the SWNT-Is (22.7 wt %) was determined by elemental analysis.

Preparation of the PMMA–SWNT nanocomposites

The SWNT-based PMMA nanocomposites were prepared by *in situ* polymerization in a solution. MMA monomer (20 mL) and the SWNT-Is (96.4 mg) were sonicated in 10 mL of THF for 3 h at room temperature. The reaction flask and reaction mixture were purged with dried N_2 for 1 h before they were immersed in a silicon oil bath at a reaction temperature of 60°C. Polymerization was carried out with continuous stirring for 24 h under the protection of an N_2 atmosphere. The reaction was terminated by the addition of an acidified methanol solution. The polymer was precipitated and dried under a vacuum at 60°C for 24 h. The PMMA-grafted nanotube (PMMA-*g*-SWNT) was separated from the polymer matrix by refluxing in THF for 24 h, repeated washing with THF, and finally, vacuum filtration through a 0.2-μm Teflon membrane. The final product of the PMMA-*g*-SWNT composite, free of ungrafted PMMA, was dried overnight *in vacuo.*

In addition, pure PMMA was prepared by a free-radical initiator [4,4′-azobis(4-cyanovaleric acid)]: 20 mL of the MMA monomer and 10 mL of THF, along with 0.12 wt % of the free-radical initiator, were added to a reactor. The reaction solution was purged with dried N_2 for 1 h. Other procedures were same as for the polymerization of the PMMA–SWNT composites.

A control sample (a PMMA–SWNT blend) was made by the sonication of a mixture of neat PMMA and SWNT-OHs in chloroform. For accurate comparisons, the same loading of SWNTs to PMMA, as in the case of the PMMA–SWNT composites, was used.

Characterization

Fourier transform infrared (FTIR) spectra were obtained with a MAGNA-IR 560 (Madison, WI) with a resolution of 4.0 cm^{-1} at room temperature. The KBr pellet method was used. The viscosity measurements were performed in a benzene solution with an Ubbelohde capillary viscometer at 25°C. The average molecular weight was calculated with the Mark–Houwink relation:[28] $[\eta] = 0.55 \times 10^{-4} M_\eta^{0.76}$, where M_η is the viscosity-average molecular weight. A Nanoindentor Snstron8848 was used for the measurement of the Young's modulus of the neat PMMA and SWNT–PMMA composites. Scanning electron microscopy (SEM) observations were performed with a LEO 1455 VP microscope (Cambridge, England) with samples being mounted on aluminum stubs with an adhesive carbon tape and then gold-coated in a sputter coater. A transmission

electron microscope (Phillips CM20) operated at an acceleration voltage of 120 kV was used to observe microstructures of the samples. The glass-transition temperature (T_g) was determined with a TA2000 differential scanning calorimeter at a heating rate of 10°C/min from 30 to 200°C. Two continuous scanning cycles were performed to remove the influence of the thermal history; the data obtained from the second scanning were accepted. The thermal decomposition temperature (T_d) was determined by thermogravimetric analysis (TGA) in a temperature range from 40 to 900°C at a scanning rate of 20°C/min under the protection of N_2 flow. The dynamic properties of the nanocomposites were measured with a dual cantilever from 30 to 200°C at a heating rate of 5°C/min with a frequency of 1 Hz. The samples were molded to a size of 10 × 30 × 2 mm^3 at 200°C for 10 min at 4000 psi.

RESULTS AND DISCUSSION

Immobilization of the free-radical initiator onto the SWNT-OHs

After treatment with the difunctional free-radical initiator, the surfaces of the SWNTs were covalently bound to species of radical initiator as follows:

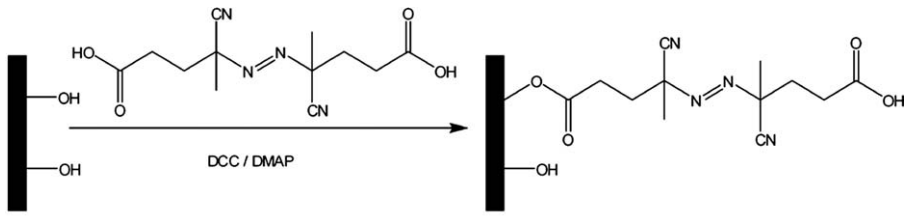

The thermal properties of the SWNT-OHs, radical initiator [4,4′-azobis (4-cyanovaleric acid)], and SWNT-Is were studied by TGA, as shown in Figure 1. The SWNT-OHs showed a high thermal stability. The total weight loss was only 3.80 wt % at 900°C. This small percentage of weight loss corresponded to the removal of the hydroxyl group on the outer surfaces of the SWNTs (3.96 wt %). On the other hand, the pure initiator underwent a dramatic weight loss around 125°C; this indicated the decomposition of the azo group and the evolution of N_2; the initiator further decomposed over the experiment temperature range. As expected, the SWNT-Is showed a rapid decomposition at the same temperature as the initiator and then a similar degradation profile to that of the pure initiator; this indicated that the initiator was attached to the surfaces of the SWNTs. The total weight loss of the SWNT-Is was 26.0 wt % at 900°C; this supported the conclusion that the content of the attached initiators and remaining hydroxyl groups was about 26.0 wt %. However, elemental analysis showed that the initiator attached to the surfaces of the SWNTs accounted for 22.7 wt % of the content. We calculated that 34.8% of OH groups on the SWNT-OHs had reacted with the free-radical initiator.

FTIR analysis further confirmed the existence of free-radical initiators on the surfaces of the SWNTs. The IR spectrum of the SWNT-OHs [Fig. 2(a)] showed a strong absorbance at 3300–3600 cm^{-1} due to the hydroxyl group on the surfaces of the SWNTs, and C=C functional groups appeared at 1600 cm^{-1}. However, as expected, the spectra of the SWNT-Is [Fig. 2(b)] showed the initiator characteristic absorption peak of the C—H bond at 3060–2900 cm^{-1}, the C=O (esteric group) bond at 1720 cm^{-1}, the C≡N (nitrile) bond at 2243 cm^{-1}, and the C—O bond at 1300–1000 cm^{-1}. In the IR spectrum of the SWNT-Is, the presence of the characteristic group frequencies of both the initiator and the SWNTs were found. The existence of the ester carbonyl band indicated that the initiators were covalently bound to the SWNTs, not just physically adsorbed on the sidewalls of the SWNTs.

Free-radical polymerization of MMA from the SWNT-Is

The free-radical polymerization of MMA was carried out in THF at 60°C with the initiator plus the MMA monomer in a 0.12% weight ratio, as shown in Table I. The MMA polymerization with the SWNT-Is as an initiator showed a low conversion (23.5%) compared to that of the pure initiator (75.0%), and the molecular weight of PMMA in its SWNT composites was greater than that in neat PMMA. Generally, every initiator molecule could produce two radicals for the MMA polymerization. However, every initiator molecule attached on the SWNTs may have produced fewer than two radicals because of the SWNT effects. So, the molecular weight of SWNT–PMMA was larger than that of neat PMMA, and a low conversion of MMA polymerization with SWNT-Is was observed. The extraction of PMMA chains from the PMMA–SWNT composites was carried out with

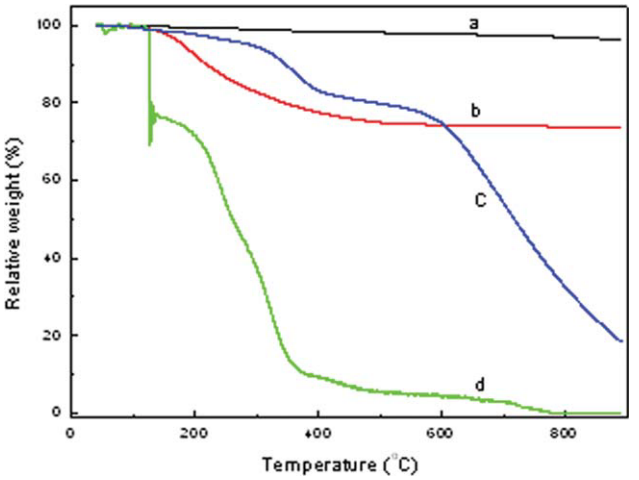

Figure 1 TGA curves of the (a) SWNT-OHs, (b) SWNT-Is, (c) SWNT-*g*-PMMA, and (d) radical initiator [4,4′-azobis (4-cyanovaleric acid)]. [Color figure can be viewed in the online issue, which is available at wileyonlinelibrary.com.]

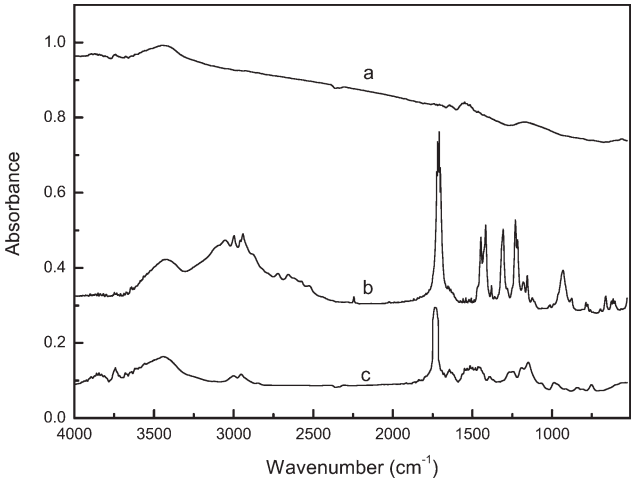

Figure 2 FTIR spectra of the (a) SWNT-OHs, (b) SWNT-Is, and (c) SWNT-*g*-PMMA.

THF refluxing in a soxhlet extractor for 24 h. The results show that only a fraction of the PMMA was extracted, whereas the neat PMMA initiated by the pure initiator was totally extracted; this indicated that the PMMA chains in its SWNT composite were attached to the surface of the SWNTs. Because the initiator was attached to the surface of the SWNTs, the PMMA chains connected the SWNTs by initiator radicals. When PMMA attached to the SWNTs, it could not completely dissolve by THF because the PMMA chain motion was restrained by interfacial interaction between the PMMA chains and the SWNTs. The size of the filter in the extractor was smaller than the size of the nanotube, so the undissolved composites could not pass through the filter. As shown in Figure 1(c), the TGA curve of SWNT-*g*-PMMA (free from neat PMMA) gave a residual weight of 18.3% at 900°C, which was ascribed to the residual SWNTs because all of the initiator moieties and the polymer (PMMA) were believed to be thermally consumed before 900°C. As a result, the content of PMMA in composite was calculated to be 81.7 wt %. In addition, the peaks in the IR spectrum of SWNT-*g*-PMMA [Fig. 2(c)] were clearly assigned to the C—H bond at 3020–2900 cm^{-1}, the esteric group bond at 1731 cm^{-1}, and the C—O bond at 1300–1000 cm^{-1}; this indicated the presence of PMMA chains in the PMMA–SWNT composite.

Microstructures of the PMMA–SWNT composites

The microstructures of the PMMA–SWNT composites were further studied by SEM and transmission electron microscopy (TEM). As shown in Figure 3(a), the pristine SWNT-OHs existed as bundles or ropes with a wide diameter distribution. Figure 3(b) shows an image of the dispersion of the nanotubes in their PMMA matrix; the carbon nanotubes were embedded and tightly held in the PMMA matrix. Some polymers were coated on the surface of the SWNT. The SWNTs were considered to have good wettability for PMMA. The lack of compatibility may have led to some agglomerated SWNT clusters. The TEM observation revealed that the SWNT-OHs existed in big bundles or ropes, whereas the carbon nanotubes in the PMMA–SWNT composite remained in smaller bundles or were separated, as shown in the high-resolution TEM images in Figure 4(a,b). The SWNT size increased because the SWNTs were coated in PMMA chains. Therefore, the SWNTs were not simply mixed up or blended with the PMMA, but they were rather glued or bound by the PMMA chains. These results indicate that PMMA could be grafted

TABLE I
Polymerization Results for MMA Catalyzed with the Initiator Only and with SWNT-Is

Run	Initiator	Conversion (%)	SWNT fraction (wt %)	Extracted by THF (%)	M_η ($\times 10^{-5}$)
1	I[a]	75.0	0	100	1.1
2	SWNT-Is	23.5	2.17	79.3	1.4

Polymerization conditions: [Initiator]/[Monomer] = 0.12% (weight ratio), 10 mL of THF as the solvent, 20 mL of MMA as the monomer, temperature = 60°C, and polymerization time = 24 h.

[a] 4,4′-Azobis(4-cyanovaleric acid) as the initiator.

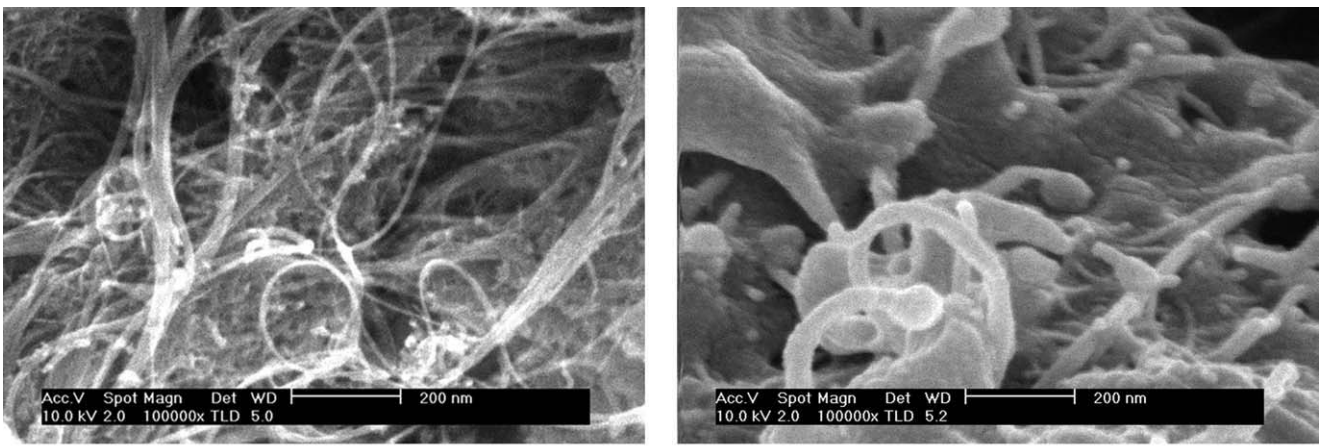

Figure 3 SEM images of the (a) pristine SWNT-OHs and (b) PMMA–SWNT composites.

through free-radical polymerization onto the surfaces of the SWNTs.

Solubility and thermal properties of the PMMA–SWNT composites

The solubility of the PMMA–SWNT composites (covalently grafted) and PMMA–SWNT blend in a $CHCl_3$ solution was also investigated. The SWNTs were not likely to be dispersed in the $CHCl_3$ solvent. The SWNTs (2 mg) in 10 mL of $CHCl_3$ were sonicated for 60 min, but sedimentation appeared 1 h after the sonication was halted, as shown in Figure 5(a). The PMMA–SWNT blend showed a result similar to that of the SWNT-OHs, as shown in Figure 5(b); this indicated poor interaction between the SWNTs and PMMA chains. However, the PMMA–SWNT composites (covalently grafted) were homogeneously dispersed in the $CHCl_3$ solvent. As Figure 5(c) shows, 2 mg of the PMMA–SWNT composites were dispersed in 10 mL of $CHCl_3$ with the aid of sonication for 60 min; no nanotube precipitation from this solution was observed, even 10 days after the sonication was ceased. Therefore, it was not difficult for us to conclude that the PMMA–SWNT composites synthesized by free-radical polymerization significantly enhanced the homogeneous dispersability of the SWNTs in organic solvents.

The thermal properties of the PMMA–SWNT composites were measured by differential scanning calorimetry (DSC) and TGA, as shown in Figures 6 and 7. The addition of the SWNTs increased the T_g values; T_g increased from 125.5°C (for neat PMMA) to 131.5°C (for the PMMA–SWNT composite) with an SWNT concentration of 2.17 wt %. Also, the control sample, PMMA–SWNT blend, had a T_g value (125.6°C) lower than that of the PMMA–SWNT composites; this indicated that poor interaction between the SWNTs and PMMA in the control sample could not improve T_g of the PMMA. The T_g value represented the extent of macromolecular segment motion. Intimate interaction between the SWNTs and the PMMA covalently attached to the surfaces of the nanotubes resulted in a decrease in the mobility of the polymer chains. In fact, the attachment of the PMMA chains to the surfaces of the SWNTs provided strong interfacial adhesion between polymer chains and nanotubes; as a result, the macromolecular segment motion was confined; this resulted in an increase in T_g.[29] Figure 7 shows the thermal stability of the neat PMMA, PMMA–SWNT blend, and the PMMA–SWNT nanocomposite (covalently grafted). The temperature for 5% weight loss was defined as T_d.[30] By comparing the curves of the PMMA–SWNT composites (T_d = 336.6°C) with that of neat PMMA (T_d = 280.0°C), we found that the T_d of the nanocomposites was 56.6°C higher than that of the neat PMMA; this indicated that the embedding of the SWNTs into the polymer matrix also improved the thermal stability of the PMMA, as reported by another group.[16,31] The increase in T_d was attributed to the interaction between the polymer chains and the surfaces of the SWNTs. On the contrary, the T_d of the PMMA–SWNT blend (296.1°C) was much lower than that of the PMMA–SWNT composites, although it was 16.1°C higher than that of the neat PMMA. The thermal dynamics of the PMMA–SWNT blend were also attributed to the interaction between the polymer chains and the SWNTs. As shown in Figure 5(b), interaction existed between PMMA and the SWNTs for certain, although the SWNTs were not efficiently dispersed in their blend.

Dynamic mechanical properties of the PMMA–SWNT composites

Dynamic mechanical thermal analysis measures the response of a given material to cyclic deformation as a function of temperature. The temperature dependence of the storage modulus (E') and tan δ are

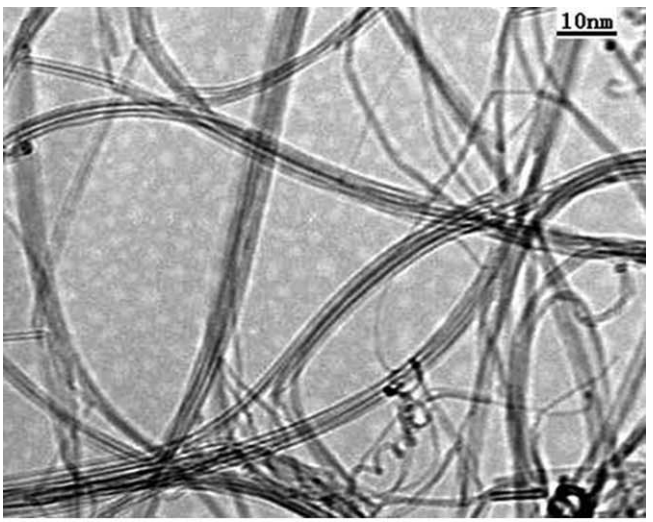

(a)

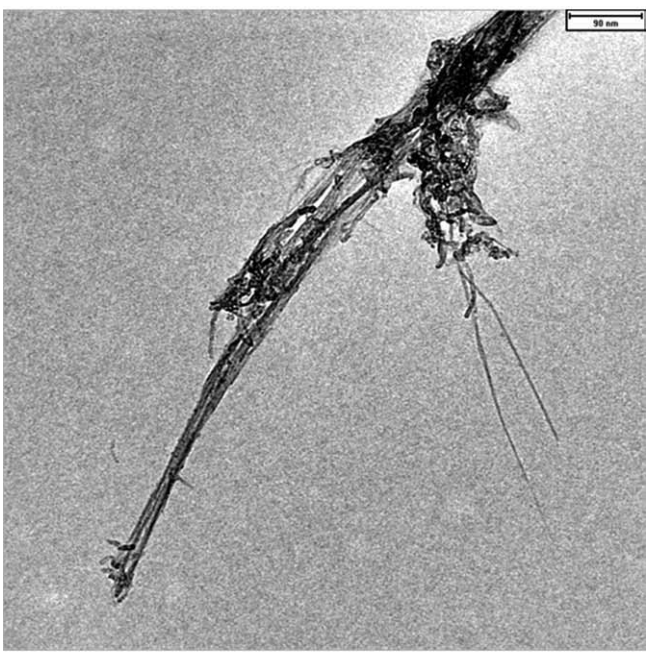

(b)

Figure 4 TEM images of the (a) pristine SWNT-OHs and (b) PMMA–SWNT composites.

shown in Figures 8 and 9, respectively. E' of a polymer decreases rapidly, whereas tan δ goes through a maximum when the polymer is heated through the glass-transition region. The maximum of tan δ is commonly taken as T_g. In both the glassy and rubbery regions, E' of the PMMA–SWNT composites was much greater than those of the neat PMMA and PMMA–SWNT blend. E' of PMMA increased by the stiffening effect of the covalently introduced nanotubes; the effect was more significant at higher temperatures. Moreover, it was higher than that of the multiwalled carbon nanotube–PMMA composites prepared by a melt-processing method,[32] although a

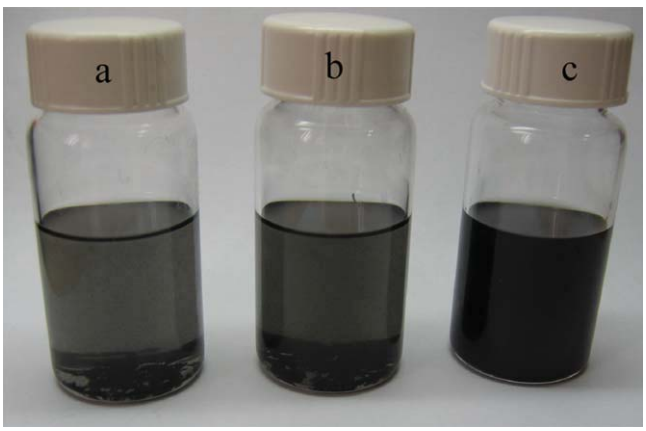

Figure 5 Stability in $CHCl_3$ (after sonication for 60 min) of the (a) pristine SWNT-OHs (time = 1 h), (b) PMMA–SWNT blend with 2.17 wt% SWNTs (time = 1 h), and (c) PMMA–SWNT composites with 2.17 wt % SWNTs (time = 10 days). The content of SWNTs in each of the bottles was 0.2 mg/mL. [Color figure can be viewed in the online issue, which is available at wileyonlinelibrary.com.]

very low SWNT content was embedded in the PMMA matrix in our case. It was interesting that the PMMA–SWNT blend showed dynamic mechanical behavior different from that of the neat PMMA with a slightly higher E' in the glassy region and a much higher E' in the rubbery region. This result indicates that the presence of carbon nanotubes in the PMMA–SWNT blend also enabled the matrix to sustain a high modulus value to higher temperature. Figure 9 shows the tan δ peaks of various samples. Peaks from the PMMA–SWNT composites and PMMA–SWNT blend obviously shifted to higher temperatures compared to that of the neat PMMA; this indicated that the T_g of the composite increased with the addition of the nanotubes. The relationship between T_g and the SWNTs in the PMMA matrix was consistent with that shown by the DSC results.

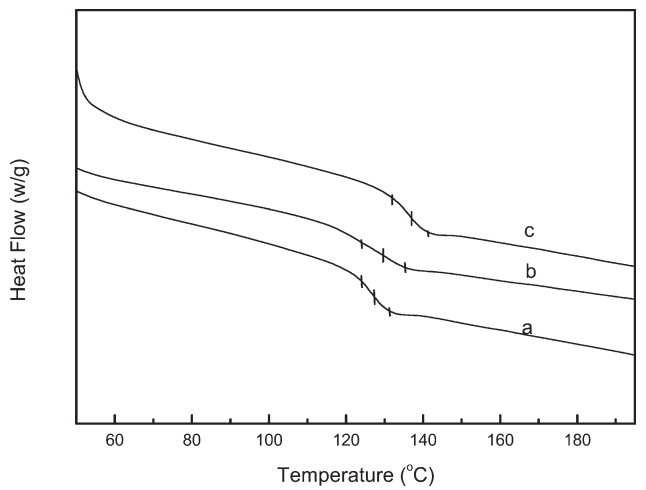

Figure 6 DSC thermograms of the (a) neat PMMA, (b) PMMA–SWNT blend, and (c) PMMA–SWNT composites.

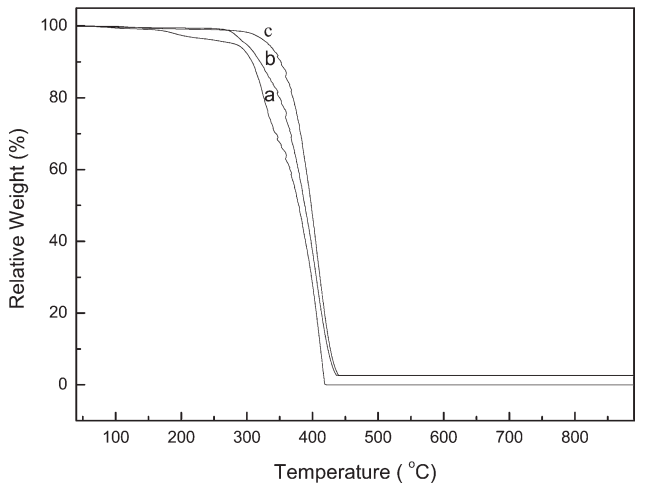

Figure 7 TGA thermograms of the weight loss as a function of temperature for the (a) neat PMMA, (b) PMMA–SWNT blend, and (c) PMMA–SWNT composites.

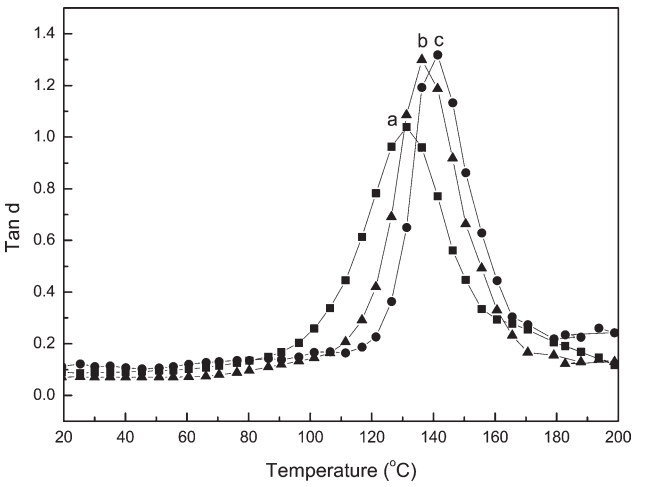

Figure 9 Tan δ versus temperature for the (a) neat PMMA, (b) PMMA–SWNT blend, and (c) PMMA–SWNT composites.

CONCLUSIONS

An *in situ* radical polymerization grafting-from approach was successfully applied to functionalize SWNTs; this resulted in SWNTs grafted with PMMA layers. Significantly, the approach can be extended to other polymers to obtain functionalized SWNTs, and researchers may explore and synthesize novel carbon-nanotube-based nanomaterials and molecular devices with tailor-made structures and properties. Because of the grafting nature of PMMA, the SWNTs could be more uniformly dispersed in the PMMA matrix than a composite prepared from a PMMA solution. Thus, carbon nanotubes played a reinforcement role in the PMMA matrix. The results obtained demonstrate that T_g, T_d, and the mechanical properties of the PMMA–SWNT increased evidently.

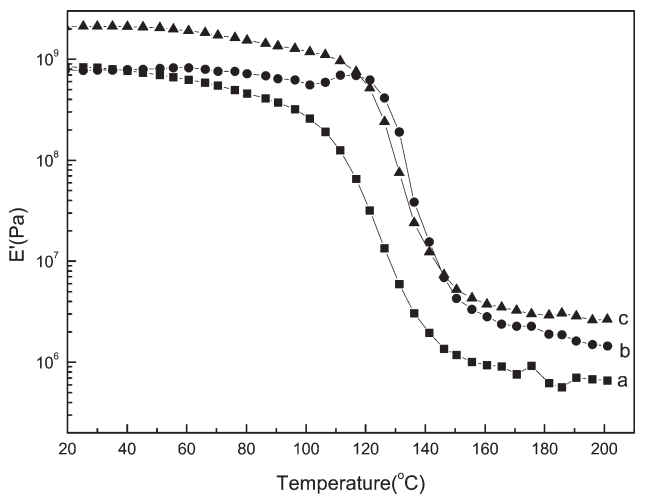

Figure 8 Trends of E' versus temperature for the (a) neat PMMA, (b) PMMA–SWNT blend, and (c) PMMA–SWNT composites.

References

1. Giannelis, E. P. Adv Mater 1996, 8, 29.
2. Shaffer, M. S. P.; Windle, A. H. Adv Mater 1999, 11, 937.
3. Bharadwaj, R. K. Macromolecules 2001, 34, 9189.
4. Ray, S. S.; Okamoto, M. Prog Polym Sci 2003, 28, 1539.
5. Ounaies, Z.; Park, C.; Wise, K. E.; Siochi, E. J.; Harrison, J. S. Compos Sci Technol 2003, 63, 1637.
6. Cui, L.; Tarte, N. H.; Woo, S. I. Macromolecules 2008, 41, 4268.
7. Cui, L.; Tarte, N. H.; Woo, S. I. J Appl Polym Sci 2008, 110, 784.
8. Iijima, S. Nature 1991, 354, 56.
9. Baughman, R. H.; Zakhidov, A.; Heer, W. A. Science 2002, 297, 787.
10. Ajayan, P. M. Chem Rev 1999, 99, 1787.
11. Treacy, M. M. J.; Ebbesen, T. W.; Gibson, J. M. Nature 1996, 381, 678.
12. Yu, M.; Lourie, O.; Dyer, M. J.; Kelly, T. F.; Ruoff, R. S. Science 2000, 287, 637.
13. Dalton, A. B.; Collins, S.; Munoz, E.; Razal, J. M.; Ebron, V. H.; Ferraris, J. P.; Coleman, J. N.; Kim, B. G.; Baughman, R. H. Nature 2003, 423, 703.
14. Bahr, J. L.; Mickelson, E. T.; Bonikowsk, M. J.; Smalley, R. E.; Tour, J. M. Chem Commun 2001, 2, 193.
15. Stephan, C.; Nguyen, T. P.; Lamy de la Chapelle, M.; Lefrant, S.; Journet, C.; Bernier, P. Synth Met 2000, 108, 139.
16. Du, F. M.; Fischer, J. E.; Winey, K. I. J Polym Sci Part B: Polym Phys 2003, 41, 3333.
17. Gorga, R. E.; Cohen, R. E. J Polym Sci Part B: Polym Phys 2004, 42, 2690.
18. Velasco-Santos, C.; Martinez-Hernandez, A. L.; Fisher, F.; Ruoff, R.; Castano, V. M. J Phys D 2003, 35, 1423.
19. Hsiao, C. C.; Lin, T. S.; Cheng, L. Y.; Ma, C. C. M.; Yang, A. C. M. Macromolecules 2005, 38, 4811.
20. Liu, L.; Barber, A. H.; Nuriel, S.; Wagner, H. D. Adv Funct Mater 2005, 15, 975.
21. Park, S. J.; Cho, M. S.; Lim, S. T.; Choi, H. J.; Jhon, M. S. Macromol Rapid Commun 2003, 24, 1070.
22. Sung, J. H.; Kim, H. S.; Jin, H.-J.; Choi, H. J.; Chin, I.-J. Macromolecules 2004, 37, 9899.

23. Park, S. J.; Lim, S. T.; Cho, M. S.; Kim, H. M.; Joo, J.; Choi, H. J. Curr Appl Phys 2005, 5, 302.
24. Clayton, L. M.; Sikder, A. K.; Kumar, A.; Cinke, M.; Meyyappan, M.; Gerasimov, T. G.; Harmon, J. P. Adv Funct Mater 2005, 15, 101.
25. Blond, D.; Barron, V.; Ruether, M.; Ryan, K. P.; Nicolosi, V.; Blau, W. J.; Coleman, J. N. Adv Funct Mater 2006, 16, 1608.
26. Yao, X.; Wu, H. X.; Wang, J.; Qu, S.; Chen, G. Chem—Eur J 2007, 13, 846.
27. Neises, B.; Steglich, W. Angew Chem Int Ed 1978, 17, 522.
28. Yang, F.; Nelson, G. L. J Appl Polym Sci 2004, 91, 3844.
29. Wang, M.; Pramoda, K. P.; Goh, S. H. Carbon 2006, 44, 613.
30. Zhao, C. G.; Qin, H. L.; Gong, F. L.; Fen, M.; Zhang, S. M.; Yang, M. S. Polym Degrad Stab 2005, 87, 183.
31. Dai, J.; Wang, Q.; Li, W.; Wei, Z.; Xu, G. Mater Lett 2007, 61, 27.
32. Jin, Z.; Pramoda, K. P.; Xu, G.; Goh, S. H. Chem Phys Lett 2001, 337, 43.